COMSOL
CONFERENCE
2024 FLORENCE

Analysis of the stress and load distribution of a bolt with threaded contact modeled in 3D

C. Hollenbeck[1] ✉ christoph.hollenbeck@bollfilter.com
1. Boll & Kirch Filterbau GmbH, 50170 Kerpen, NRW, Germany

Abstract

A bolt connection can be modeled and simulated in different ways. In many engineering cases, only the stresses in and the contact pressure between bolted parts of an assembly are of interest. Here in this work, a bolt with thread and matching screw nut has been modeled in 3D in order to simulate the load distribution of the 3D thread contact. This is numerically challenging, because mechanical contact modeling can be a geometrically highly nonlinear problem especially with this helical contact of the threads. For this reason, numerical stabilization methods were applied. The module "Solid Mechanics" has been applied for an assembly and the contact method chosen was "Augmented Lagrangian" as the most accurate method for determining contact pressure. The system has been meshed relatively finely to resolve the geometry with the fillets resp. root radii at the bases of the thread. In addition, the contact surfaces have been finely meshed so that the most accurate surface pressure profile possible can be simulated. This has led to the fact, that of lot of temporary memory (RAM) and PC-side calculation time has been required. Cloud computing has been used for this purpose. The goal of this work is to determine reliable results of the stress and contact pressure distribution of the described bolted joint using studies that are as accurate as possible in terms of the geometry. In for example Roloff/Matek as generally recognized technical literature, a load share of approximately one third or 33 % of the first thread of six threads engaged in total is displayed besides a shown load distribution. This is compared with the simulation results of this study and the results differ significantly. Descriptive and illustrative reasons are presented in the evaluation.

Keywords: FEM, FEA, bolt with 3D thread, threaded contact, mechanical contact, load distribution, Lagrange multiplier, Augmented Lagrangian, notch effect, stress concentration

Introduction

An overview to the topic is given above in the abstract. In accordance with VDI Guideline 2230 Sheet 2, simulations are performed here in 3D according to model class IV as the most accurate and numerically demanding model class. This simulation is numerically very challenging because the bolt is not fully constrained in its degrees of freedom of motion in this static study unless additional measures are taken. A crucial modeling method is described in the chapter ‚Numerical Model‘.

Geometrical Set Up

At the beginning, a bolt of the type M12 was designed (see *Figure 1*). The thread of this bolt does contain root radii resp. core fillets. Theoretically, an M12-screw might have a diameter of exactly 12 mm, but it is normally smaller due to common tolerances. Here a diameter of the bolt with 11.9 mm has been chosen. This diameter is within the tolerance field '6h' with a minimum to maximum dimension of 11.735 mm to 12 mm. This diameter is also within the tolerance field '6g' with a minimum to maximum dimension of 11.701 mm to 11.966 mm. The corresponding root radii are $r_{bolt} = 0.253$ mm and $r_{nut} = 0.126$ mm.

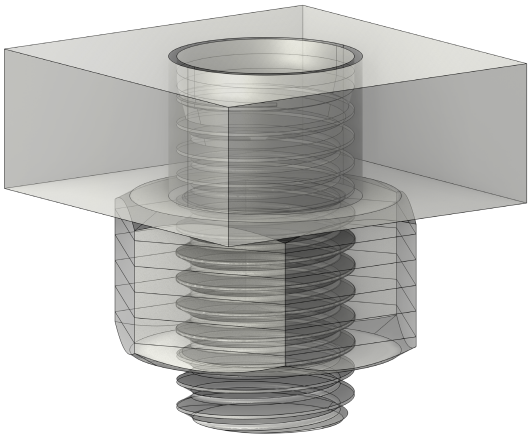

Figure 1. 3D – bolt in an assembly with a nut and a mounting block with a through hole (transparent display)

These radii are not just small geometric details, they have a very strong effect on the level of the notch effect or stress concentration. Neglecting them with an alternative, simplified constructed thread would lead to unrealistic high, local stress concentrations at sharp edges, which would then be present. For the pitch of the thread the default value of $P = 1.75$ mm

has been chosen.

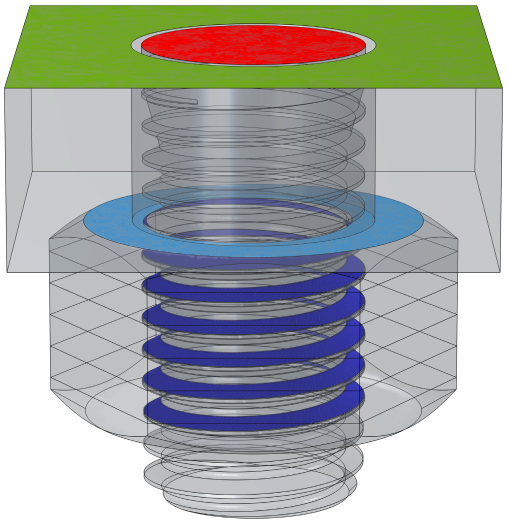

Figure 2. 3D – CAD – assembly as a basis for the simulation (with coloring of the mechanical contact pairs and the boundary conditions)

Besides the bolt this assembly contains one nut and a supporting block of metal (see *Figure 2*). The M12 bolt is positioned in this block with a through hole of the diameter $\varnothing_{hole}$ = 13 mm (as smallest resp. finest value in DIN ISO 20273). The nut has been modeled with a small chamfer of 0.25 mm in order to remove only a small portion of the first thread. The mechanical contact pairs are marked in dark blue (thread contact) and light blue (contact between nut and block).

Numerical Model

It has been simulated in a linear-elastic or materially linear manner in order to avoid making the task even more non-linear due to the high degree of geometric nonlinearity that is already present. In general, the physics "structural mechanics" has been used obviously and the studies have been simulated without friction losses. Linear elastic simulations follow the equation $\sigma = \varepsilon \cdot E$. The mechanical stress σ increases linearly as function of the strain ε, if the Young's modulus E is constant and this is the case for linear elastic studies. As material, steel with a Young's modulus of E = 200 GPa = 200 · 10^3 N/mm^2, a density of ϱ = 7850 kg/m^3 and a Poisson's ratio is ν = 0.3 is chosen. A relatively low preload force of F = 10 kN has been applied, which is appropriate for this linear elastic study. For a bolt with a strength class of e. g. 4.8 with a 0.2 % yield strength of $R_{p0.2}$ = 320 N/mm^2 the bolt utilization factor is approximately

$F_{preload} / F_{preload\_max} =$
$F_{preload} / [0.25 \cdot \pi \cdot (d_{core})^2 \cdot R_{p0.2}] =$
(10 kN) / [0.25 · π · (9.853 mm)^2 · 320 N/mm^2]
≈ 0.41 = 41 %.

The two mechanical contact pairs present are considered numerically. This is the thread contact and the contact between the nut and the block as initially flat surfaces. The simulations presented here in this work are geometrically nonlinear because of considering these contact pairs. In COMSOL®, each contact pair has a so-called source and destination. In the case of a similar stiffness with the same material, the concave part should be defined as the source and the convex part as the destination. The destination should be meshed finer compared to the source by at least a factor of two [1]. Here the destination boundary was assigned to the surface of the bolt side, which is the surface that is curved outwards or convex in certain respects. The corresponding surface of the nut was meshed coarser by a factor of 2.25 > 2.

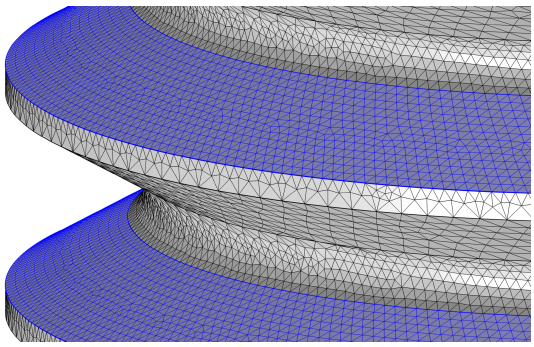

Figure 3. partial view of the FE-mesh at the bolt

The element length of the triangular finite elements at the thread contact surface on the bolt side has been set to a value of Δs = 0.1 mm = 100 µm. A number of 13 elements are positioned along the radial width of the thread (see *Figure 3*).

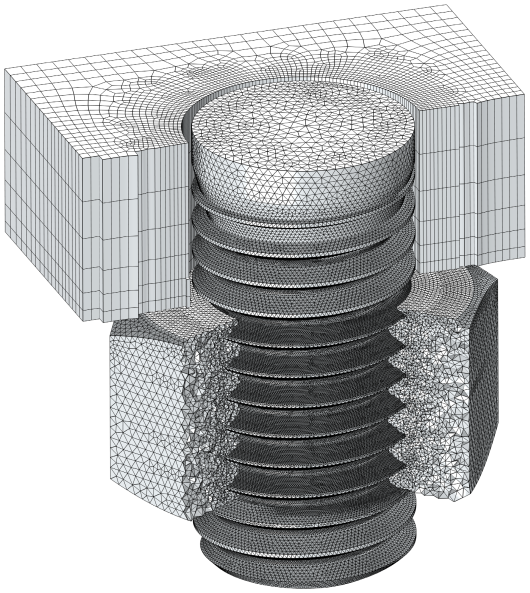

Figure 4. FE-mesh in total partly with breakouts

For a 3D simulation, a fairly fine mesh with a number of elements for the whole geometry of $n \approx$ 5.8 Mio. in total was created (see *Figure 4*).

In the metal block, to a certain extent more structured meshing was possible creating square prisms (see *Figure 4* & *Figure 5*). In the bolt and the nut, meshing was only possible using tetrahedra, especially because of the core roundings.

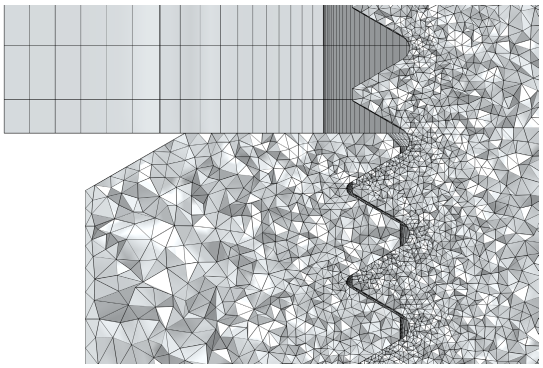

Figure 5. partial side view of FE-mesh of halved system

In [2, p. 138] it is stated, that linear [discretized] tetrahedral elements are the worst which can be chosen, because each is mechanically very stiff itself. The default setting of the discretization in structural mechanical simulations in COMSOL® is 'Quadratic serendipity' (without center nodes). On the one hand, source [2, p. 138] describes that serendipity elements have long been proven in practice; on the other hand, the same source [2, p. 241] describes and justifies that quadratic serendipity elements should not be used for contact calculations, which is why a slightly higher discretization of 'Quadratic Lagrange' has been chosen here and this is significantly higher discretized than 'linear'.

In addition, the optional settings "Calculate boundary flows" and "Apply smoothing to boundary flows" have been activated in the simulations. Both contact pairs were defined with the contact method "Augmented Lagrangian" in contrast to the less accurate "Penalty" method. In [3, p. 263] it is mentioned, that the Lagrange multiplier is the same as the contact force and in [2, p. 229] it is stated, that displacements correspond exactly to the analytical solution using the method of Lagrange Multiplier in the context of mechanical contact in FEM-studies. The initial value of the contact pressure is set to $T_n = 0$ N/m^2 for both mechanical contact pairs and this is the default value. This makes sense in combination of ramping up the preload resp. force along the axis in an auxiliary sweep beginning with a force of $F_{preload} = 0$ kN and increasing it in small steps to reach convergence. Then there are appropriate initial values available for each intermediate step in this so-called 'Continuation method'. This force is applied to the surface marked in red in *Figure 2* and acts vertically resp. upwards along the axis. The surface marked in green is fixed (see also *Figure 2*).

The 'Continuation method' with ramping up the force beginning with zero has been combined with a special modeling method. This is the method announced at the end of the ‚Introduction'. The block with its fixation at the top surface is completely constrained. The bolt and nut are not fixed in any point and unintentional rigid body motion might occur. That are displacements, which do not make any sense and geometric penetrations can also occur without respecting the contact pairs. A volumetric spring foundation feature for the bolt and nut have been applied [1]. A spring of the type “total spring constant” was assigned an initial value of $k_{spring} = 10^{14}$ N/m as spring stiffness. The variable spring stiffness was assigned to k_spring·(1-ramp_fact)·2^(-ramp_fact·5) as term in original notation of the COMSOL® - file. In the context of the 'Continuation method' mentioned above, the increase of the load resp. the force was combined with a reduction of the spring stiffness. The coupling between both has been realized with a ramping factor (“ramp_fact” in the formula). This has been increased from '0' to '1' in small steps (ramp_fact = 0 ≙ 0 kN = F_{load} and maximal, initial spring stiffness; ramp_fact = 1 ≙ 10 kN = F_{load} and zero spring stiffness).

The simulation has needed a calculation time of $\Delta t_{calc} = 85957$ s (≈ 23 h 52 min) and a physical memory requirement of 124.84 GB RAM (virtual memory: 133.28 GB). If a direct solution algorithm or equation solver had been used, even much more memory would have been required. A suggested iterative solver with ‚Algebraic Multigrid' (number of multigrid levels: 3) was therefore used. A comparison using a smaller model has shown, that a direct solver like PARDISO would have needed approximately six times more RAM (proportionally estimated in this case: 749 GB ≈ 6 · 124.84 GB). The calculations were performed with 24 virtual cores using a certain configuration of a virtual PC in the Microsoft® Azure Cloud.

Simulation Results

The contact pressure at the thread is shown directly at the beginning of the presentation of the results (see *Figure 6*). Qualitatively, the load distribution on the thread can be roughly estimated on the basis of this illustration. The quantitative values can be taken from a table (see *Table 1*). This postprocessing has been possible via
→ Derived Values
→ Surface Integration
→ Click on the contact surface
on the side of the destination
→ typing in
“if(z<-20[mm] && z>=-21.75[mm],solid.Tn,0)”
(for the 1st thread).

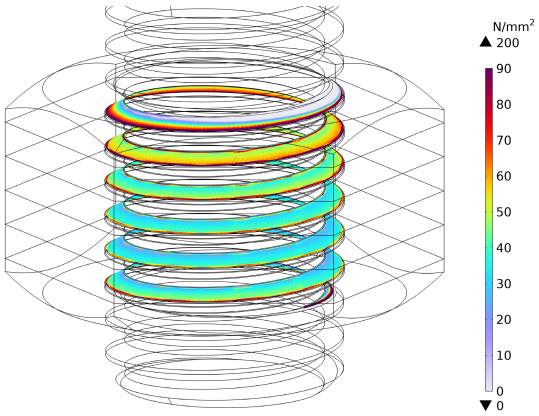

Figure 6. Contact pressure at the thread (contact pressure on the nut hidden for a better view on the thread)

Load shares of the individual threads corresponding to *Figure 6*					
1st	2nd	3rd	4th	5th	6th
20.2 %	21.4 %	16.9 %	14.1 %	12.6 %	14.8 %

Table 1: Load distribution with relative load shares

At first glance, it is quite surprising that the first thread with $\varphi_1 = 20.2$ % has a smaller load share than the second thread with $\varphi_2 = 21.4$ %. The uppermost part of the first thread has an area with a surface pressure of zero. This can be seen even better in a zoomed-in view of *Figure 6* (see *Figure 7*).

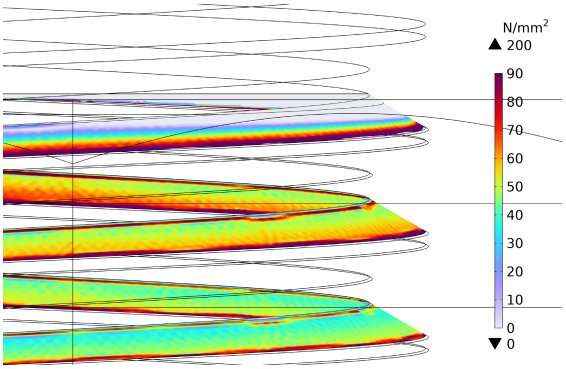

Figure 7. Part of YZ – side view of the contact pressure The horizontal lines have a distance of the thread pitch $P = 1.75$ mm.

It can be seen that there are contact pressure peaks at the edges (radially inside and outside) because the material ends abruptly on one side of the contact pair in each case. Radially inwards the nut ends and radially outwards the geometry of the bolt ends. In such cases, these peaks in the contact pressure are to expect. Before the lower load share of the first thread is explained using other results, a look is first taken at the equivalent stress according to von Mises (see *Figure 8* & *Figure 9*). Although the load share of the first thread is lower than this of the second thread, the maximal stress does occur in the root radius of the first thread (see *Figure 9*). In addition, stress concentrations due to notch effects can be seen at the core fillets of the thread.

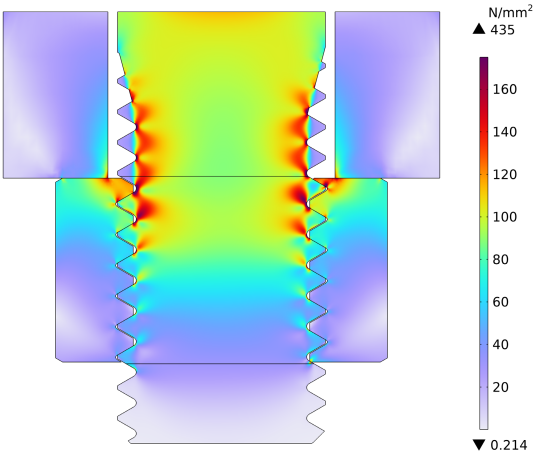

Figure 8. equivalent stress according to von Mises in the centered, vertical YZ – plane

The geometry of the nut looks different in various sectional views resp. cross sections.

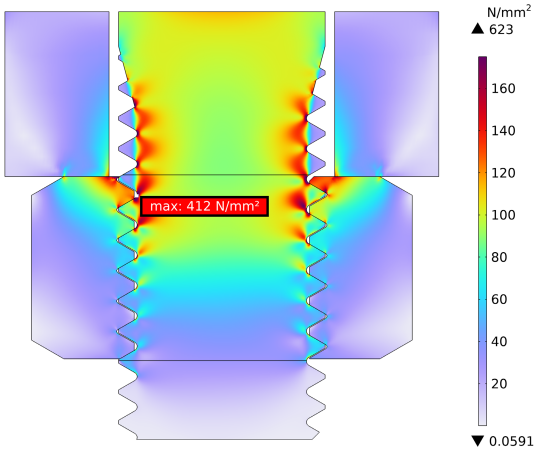

Figure 9. equivalent stress according to von Mises in the centered, vertical XZ – plane (incl. marking of the maximal stress)

In order to find an explanation for the lower load share of the first thread, one can look at a vectorial representation of the contact pressure in a sectional view (see *Figure 10*). Each cross-sectional view of this 3D thread looks different, but it is especially evident here in the upper part of the first thread that the path for the stress flow or flow of the force to the nut is very long. This leads to the result, that the contact pressure in the upper area of the first thread even decreases to zero. The contact pressure distribution can be seen in the same sectional view on the other side in *Figure 11*.

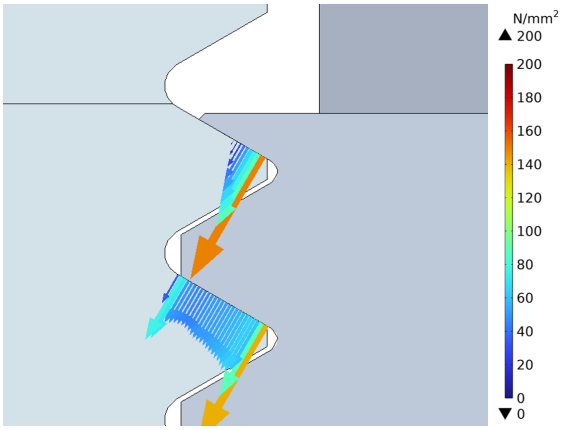

Figure 10. Vectorial illustration of the contact pressure at the thread in a sectional plane (YZ)

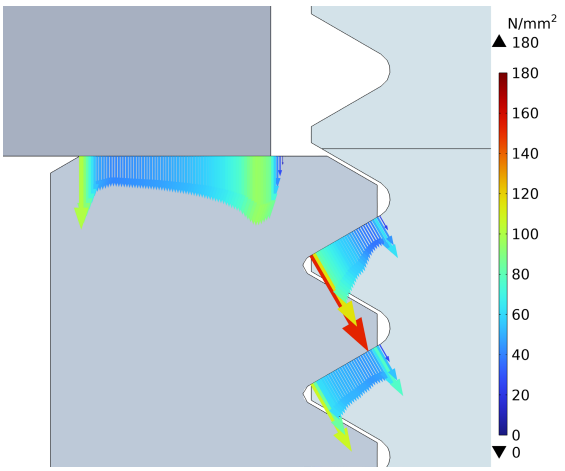

Figure 11. Vectorial illustration of the contact pressure (incl. at the nut) in the same cross section as in Figure 10 here on the left side

In an alternative, geometric simplification with a 2D axisymmetric approach, this view with a geometric mapping of a large part of the first thread (see *Figure 11*) would be sensible to choose. Then the load share of the thread would obviously be larger. In this illustration, the contact pressure at the contact between nut and block slightly extends beyond the nut, since the meshing is much coarser than the meshing of the thread. The load share of the first thread simulated here is surprisingly low.

Another simulation, essentially the same but with a much finer meshed contact zone, was carried out to exclude the possibility that this result could be due to too coarse meshing. In this mesh refinement study, the destination surface of the thread having seen in *Figure 3* has now been meshed with 42 elements along the width of the thread instead of 13 elements of the simulation described so far (16 instead of 6 elements on the source side). Besides some other details, the "maximum element groth rate" of the free tetrahedral meshing has been increased to a value of ‚2' (before 1.1) to realize a coarser meshing of the ambience of the very fine meshed contact zone. The total number of finite elements could thus be reduced to around 3.17 Mio. [with 111.83 GB RAM; $\Delta t_{calc} \approx$ 23 h 48 min] (before ≈ 5.8 Mio. elements; 124.84 GB RAM), although the contact zone is around three times as finely meshed. In the first simulation, emphasis was placed on meshing relatively uniformly with a small geometrical scale ratio as ratio between the largest and smallest finite element, because a large scale ratio might lead to numerical instabilities.

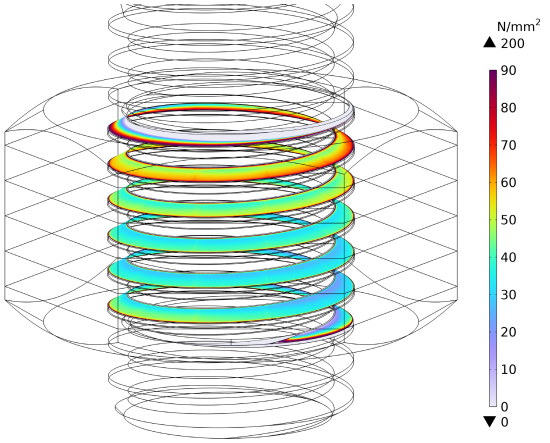

Figure 12. Contact pressure with extremely fine meshed thread contact zone (42 elements); directly comparable to the result of the coarser mesh to see in Figure 6

The contact pressure is now extremely finely resolved due to the very fine mesh used (see *Figure 12* & *Figure 13*).

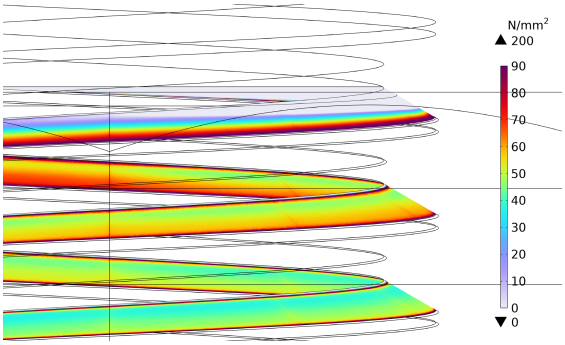

Figure 13. Contact pressure at the thread in a side view with extremely fine meshed thread contact zone (Zoom-In), directly comparable to Figure 7

A comparison of the resulting load distribution of the two different FE-meshes leads to quite small differences. Rounded to tenths of a percent, these are the same load distribution results (see *Table 1*). From this it can be concluded that the mesh initially used has already been appropriately fine but not perfectly resolved.

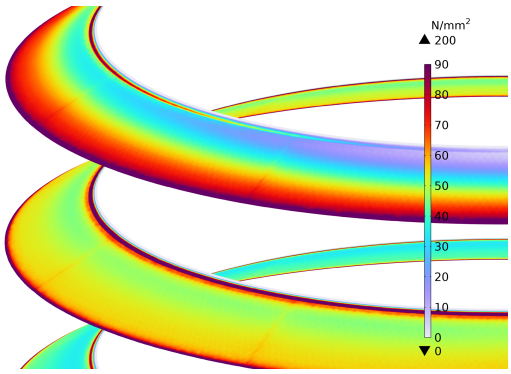

Figure 14. Detail of the contact pressure of a part of the two first threads in an angled view with extremely fine resolved thread contact zone

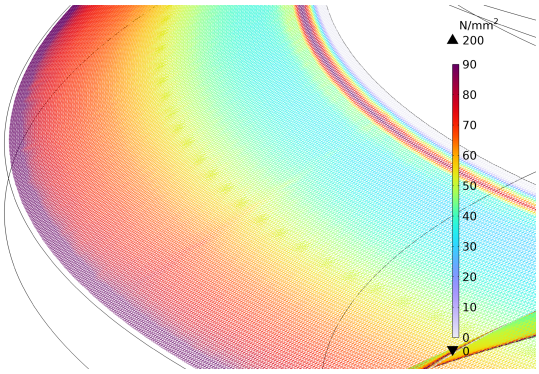

Figure 15. Very detailed view of the contact pressure in an angled view with extremely fine resolved thread contact zone: This is a zoom-in of the upper left corner of the image before (Figure 14). Wireframe rendering is activated here. In a Zoom-In of this picture in high resolution (300 dpi) the single triangles can bee seen in the digital version (PDF-file).

In *Figure 15* a part of the very fine meshed contact zone is to see. Herein there is not only to see the finite element mesh with its 42 elements along the radial width of the thread. With the chosen discretization of the type 'Quadratic Lagrange' (see chapter *Numerical Model*) all triangular elements have an additional node centered at each edge. This leads to the effect, that each triangle contains four smaller triangles. This in turn means that twice as many triangles can be seen along the radial width of the thread. That are $2 \cdot 42 = 84$ triangles.

If the diameter of the through hole were to be reduced, this load share would have to increase, especially with regard to *Figure 10* & *Figure 11*. Other authors probably have simulated with such a smaller diameter of the through hole [4]. Therefore, it seemed obvious to additionally carry out in general the same simulation, only with a change in the reduction of the diameter of the through hole.

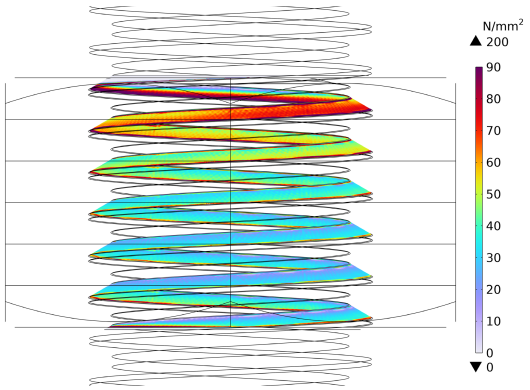

Figure 16. Contact pressure in a YZ – side view for the variant with a through-hole of 12.1 mm

The contact pressure of the variant with a through hole of $\varnothing_{hole} = 12.1$ mm is to see in *Figure 16*. Based on this simulation result image, the contact pressure can again only be estimated as having shown in *Figure 6*. The quantitative load shares can be taken from a table (see *Table 2*).

Load shares of the individual threads corresponding to *Figure 16*					
1st	2nd	3rd	4th	5th	6th
24.0 %	21.1 %	16.0 %	13.2 %	11.8 %	14.0 %

Table 2: Load distribution with relative load shares for the variant with a through hole of $\varnothing_{hole} = 12.1$ mm

In *Table 2* it is to see, that the load share of the first thread with a value of
$\varphi_1^* = 24.0$ % (for $\varnothing_{hole} = 12.1$ mm) has significantly increased in comparison to the previous value of
$\varphi_1 = 20.2$ % (for $\varnothing_{hole} = 13$ mm).

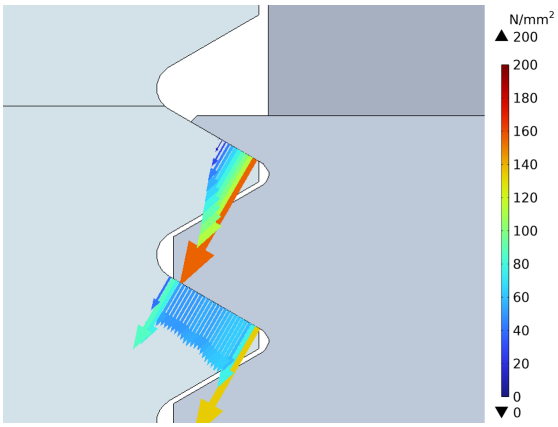

Figure 17. Vectorial illustration of the contact pressure at the thread in a sectional plane (YZ) for the variant with a through-hole of 12.1 mm *directly comparable to Figure 10 (with the same scaling)*

This difference can again be explained by the concept of stress or force flow.

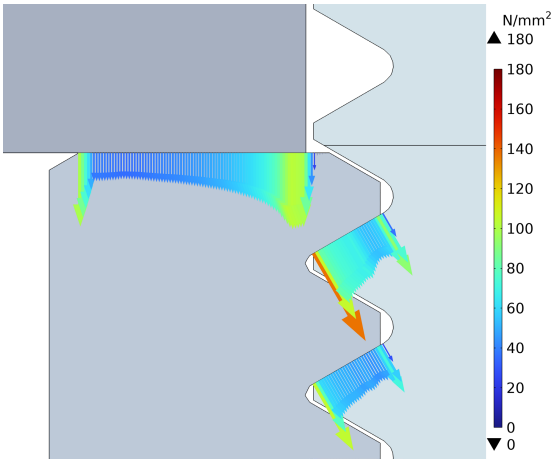

Figure 18. Vectorial illustration of the contact pressure (incl. at the nut) for the variant with a through-hole of 12.1 mm *directly comparable to Figure 11 (with the same scaling)*

The distance resp. path from the first thread to the nut is significantly shorter in the variant with a through hole diameter of 12.1 mm, so that there is more force flow through the first thread. In *Figure 17* & *Figure 18* it is to see, that the first thread has a larger load share in each case compared to the original variant with a through hole diameter of 13 mm.

Additional Studies

Additional simulations have been performed to see what the load distribution looks like for a threaded through hole. The geometry is shown in *Figure 19* with marked boundary conditions.

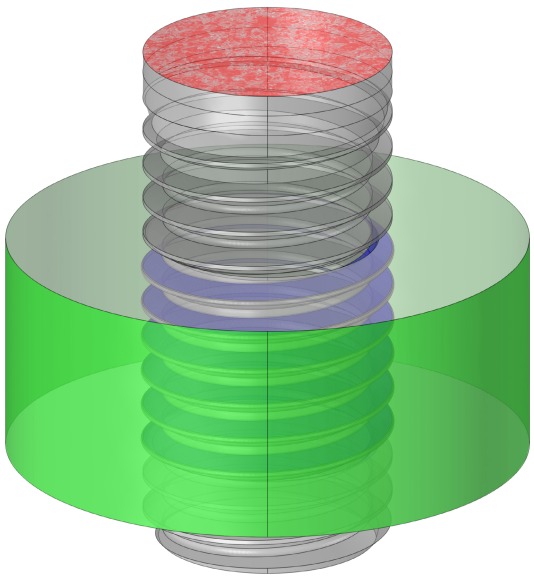

Figure 19. Bolt in threaded through hole: The fixation is marked in green and the force is applied vertically upwards to the surface marked in red.

The profile of the contact pressure and the load distribution can be seen in *Figure 20* & *Table 3*.

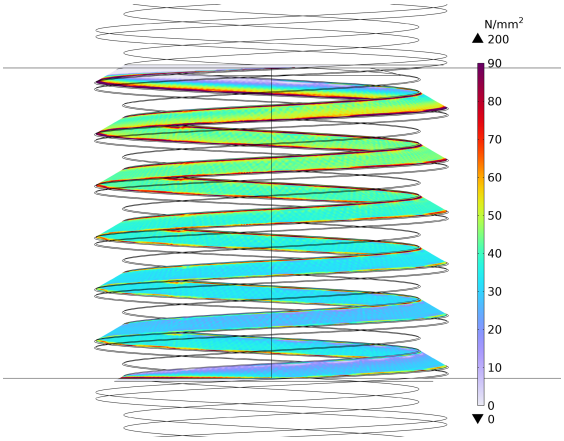

Figure 20. Contact pressure profile in a side view corresponding to the geometry displayed in Figure 19

Load shares of two variants corresponding to the geometry displayed in *Figure 19* (a) boundary conditions as shown in *Figure 19*; (b) fixation changed to the top surface of the cylinder						
	1st	2nd	3rd	4th	5th	6th
(a)	18.3 %	20.9 %	18.6 %	15.8 %	13.3 %	13.1 %
(b)	47.1 %	19.6 %	12.5 %	8.49 %	6.28 %	6.01 %

Table 3: Load distribution with relative load shares corresponding to the geometry of Figure 19

It can be seen that it makes a difference whether a screw nut is interposed as a contact body or not. The same geometry displayed in *Figure 19* has been simulated with changing the fixation from the cylindrical shell surface to the top surface of the cylinder. It is important to mention, that a fixation especially as here partially close to contact surfaces is an extreme boundary condition as a Dirichlet boundary condition with a prescribed displacement of zero.

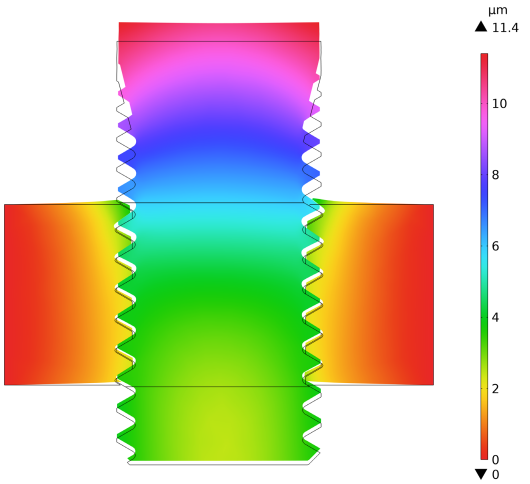

Figure 21. Display of the total displacement in a mid cross section corresponding to the geometry and the boundary conditions of Figure 19
(incl. exaggeration of the displacement by a factor of '100' to be able to see the direction)

Having changed the fixed surface, the load distribution is completely different (see *Table 3* under (b)). The fixation of the top surface does block any elastic shift. This makes the upper part of the geometry close to the first thread mechanically very stiff. Accordingly, the load share of the first thread increases significantly to a very high value of $\varphi_1 = 47.1$ %. Approximately the same result would have been expected if the support block had been omitted from the simulation shown at the beginning and the surface marked in light blue (see *Figure 2*) had been fixed instead. The total displacement for the much more realistic, initial fixation displayed in *Figure 19* is to see in *Figure 21*. Herein it is to see, that the vertical side walls are fixed, while the upper horizontal edges and the upper local area of the cylinder block can shift elastically upwards.

Conclusions

If a realistic value is used for the diameter of the through hole, the studies have shown that the first thread with a load share of $\varphi_1 = 20.2$ % even has a smaller load share than the second thread. This is mainly due to the fact that there are unfavorable conditions for the flow of force particularly in the area at the beginning of the first thread. The diagram (see *Figure 22*) shows a comparison of the load distributions stated by others and simulated here.

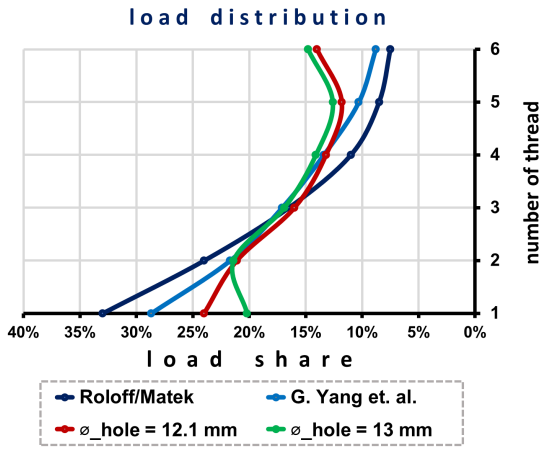

Figure 22. Diagram with different load distributions (sources: [4]; [5, p. 228])

It is also noticeable that in the load distribution simulated here, the last thread has a higher load share than the penultimate thread. This seems to be realistic because the nut ends at the last thread and the bolt continues, i. e. the material ends abruptly on one side of this contact pair. Accordingly, the force flow lines concentrate at the end of the nut, so that it can be again argued with force flow considerations here. In the same way, the one-sided ending of the material of the contact pair leads to contact pressure peaks on the thread radially on the inside and outside. The simulations here were carried out linear elastically. If materially nonlinear simulations had been used, the deviations would have been very small, especially for small and medium preload forces. This was shown by the studies presented at the COMSOL Conference in Munich 2023.

References

[1] COMSOL®, "Structural Contact Modeling Guidelines," COMSOL Multiphysics®, [Online]. Available: https://www.comsol.de/support/learning-center/article/Structural-Contact-Modeling-Guidelines-83831. [Accessed 15th August 2024].

[2] L. Nasdala, FEM-Formelsammlung Statik und Dynamik, 3rd ed., Springer Vieweg, 2015.

[3] W. Rust, Nichtlineare Finite-Elemente-Berechnungen, 3rd ed., Springer Vieweg, 2016.

[4] G. Yang and others, "Three-dimensional Finite Element Analysis of the Mechanical Properties of Helical Thread Connection," 2013.

[5] H. Wittel et. al., Roloff/Matek Maschinenelemente, Vieweg+Teubner, 2009.